

Supporting Information

Zirconium and hafnium complexes bearing pyrrolidine derived salalen-type {ONNO} ligands and their application for ring-opening polymerization of lactides

Yu-Lai Duan, Zhi-Jian Hu, Bo-Qun Yang, Fei-Fei Ding, Wei Wang, Yong Huang* and Ying Yang*

*Key Laboratory of Nonferrous Metals Chemistry and Resources Utilization of Gansu Province,
College of Chemistry and Chemical Engineering, Lanzhou University, Lanzhou 730000, Gansu, P. R.
China*

1. Table S1. Crystallographic data for complexes 1 , 3 , 4 and 5	S2
2. Table S2. Selected bond lengths (Å) and angles (°) for complexes 1 , 3 , 4 and 5	S3
3. Fig. S1. ^1H NMR spectrum of complex 1 in C_6D_6	S4
4. Fig. S2. ^{13}C NMR spectrum of complex 1 in C_6D_6	S4
5. Fig. S3. ^1H NMR spectrum of complex 2 in C_6D_6	S5
6. Fig. S4. ^{13}C NMR spectrum of complex 2 in C_6D_6	S5
7. Fig. S5. ^1H NMR spectrum of complex 3 in C_6D_6	S6
8. Fig. S6. ^{13}C NMR spectrum of complex 3 in C_6D_6	S6
9. Fig. S7. ^1H NMR spectrum of complex 4 in C_6D_6	S7
10. Fig. S8. ^{13}C NMR spectrum of complex 4 in C_6D_6	S7
11. Fig. S9. ^1H NMR spectrum of complex 5 in C_6D_6	S8
12. Fig. S10. ^{13}C NMR spectrum of complex 5 in C_6D_6	S8
13. Fig. S11. NOESY spectrum of complex 5 in C_6D_6	S9
14. Fig. S12. Variable temperature ^1H NMR spectra for complex 5 in C_7D_8	S9
15. Fig. S13. Methine region of the homonuclear-decoupled ^1H NMR spectra of isotactic PLAs at different conversions produced using initiator 5	S10
16. Fig. S14. Plot of P_m vs. conversion for polymerization of <i>rac</i> -LA with 5	S10
17. Table S3. Tetrad probabilities based on Bernoullian Statistics (Th) and experimental values (Exp) as obtained by NMR analysis.....	S11
18. Table S4. Tetrad probabilities based on Enantiomeric Site Control Statistics (Th) and experimental values (Exp) as obtained by NMR analysis.....	S11
19. Fig. S15. ESI-MS spectrum of oligomer of <i>rac</i> -lactide.....	S11

Table S1. Crystallographic data for complexes **1**, **3**, **4** and **5**.

Complex	1	3	4	5
Empirical formula	C ₄₆ H ₅₈ N ₄ O ₄ Zr	C ₃₉ H ₅₈ N ₄ O ₄ Hf	C ₄₀ H ₆₀ N ₄ O ₄ Zr	C ₄₀ H ₆₀ N ₄ O ₄ Hf
Formula weight	822.18	825.38	752.14	839.41
Temperature (K)	293(2)	293(2)	293(2)	293(2)
Wavelength (Å)	0.71073	0.71073	0.71073	0.71073
Crystal system	Orthorhombic	Monoclinic	Monoclinic	Monoclinic
Space group	P 2 ₁ 2 ₁ 2 ₁	P 2 ₁	P 2 ₁	P 2 ₁
Unit cell dimensions				
a (Å)	11.329(2)	10.9194(2)	11.0439(3)	11.01520(14)
b (Å)	17.763(4)	10.6543(2)	10.3438(3)	10.33345(14)
c (Å)	22.61(4)	16.9439(4)	17.7240(5)	17.7349(2)
α (°)	90	90	90	90
β (°)	90	99.216(2)	99.103(3)	99.2001(13)
γ (°)	90	90	90	90
V (Å ³)	4550.4(15)	1945.77(7)	1999.21(9)	1992.70(5)
Z	4	2	2	2
Calculated density (g/cm ³)	1.200	1.409	1.249	1.399
Absorption coefficient (mm ⁻¹)	0.285	2.723	0.318	
F(000)	1736	848	800	864
Crystal size (mm)	0.22 x 0.18 x 0.15	0.23 x 0.18 x 0.12	0.25 x 0.22 x 0.18	0.22 x 0.18 x 0.16
θ range for data collection (°)	3.43 to 24.99	3.31 to 25.00	3.49 to 25.00	3.38 to 24.99
Index ranges	-6<=h<=13 -20<=k<=21 -24<=l<=26	-7<=h<=12 -7<=k<=12 -19<=l<=20	-13<=h<=11 -6<=k<=12 -21<=l<=21	-13<=h<=7 -12<=k<=12 -21<=l<=20
Reflections collected	17693	7114	7417	7021
Independent reflections	7987	5153	5073	5655
R _{int}	0.0401	0.0258	0.0343	0.0233
Completeness to θ (%)	99.7	99.7	99.7	99.7
Data / restraints / parameters	7987/12/514	5153/49/433	5073/2/442	5655/25/442
Goodness-of-fit on F ²	1.005	1.001	1.002	1.006
Final R indices [I>2sigma(I)]	R ₁ = 0.0509 wR ₂ = 0.1090	R ₁ = 0.0270 wR ₂ = 0.0581	R ₁ = 0.0400 wR ₂ = 0.0712	R ₁ = 0.0245 wR ₂ = 0.0511
R indices (all data)	R ₁ = 0.0623 wR ₂ = 0.1146	R ₁ = 0.0301 wR ₂ = 0.0602	R ₁ = 0.0466 wR ₂ = 0.0757	R ₁ = 0.0266 wR ₂ = 0.0523

Largest diff. peak and hole (e. Å ⁻³)	0.572 and -0.417	0.730 and -0.681	0.390 and -0.337	0.500 and -0.391
---------------------------------------------------	------------------	------------------	------------------	------------------

Table S2. Selected bond lengths (Å) and angles (°) for complexes **1**, **3**, **4** and **5**.

Complex	1 (M = Zr)	3 (M = Hf)	4 (M = Zr)	5 (M = Hf)
M(1)-O(1)	2.163(3)	2.138(5)	2.158(3)	2.139(5)
M(1)-O(2)	2.030(3)	2.017(4)	2.021(3)	2.010(3)
M(1)-O(3)	1.939(3)	1.915(6)	1.927(3)	1.917(5)
M(1)-O(4)	1.915(3)	1.920(3)	1.926(3)	1.919(3)
M(1)-N(3)	2.352(4)	2.304(5)	2.345(4)	2.308(4)
M(1)-N(4)	2.451(4)	2.416(4)	2.451(3)	2.420(3)
O(1)-M(1)-N(3)	76.85(13)	78.2(2)	76.82(13)	77.29(16)
O(1)-M(1)-N(4)	95.86(12)	100.0(2)	98.55(13)	98.37(19)
O(2)-M(1)-O(1)	165.83(13)	166.97(19)	165.86(13)	166.31(16)
O(2)-M(1)-N(3)	89.10(14)	88.82(19)	89.04(13)	89.03(15)
O(2)-M(1)-N(4)	77.33(13)	76.65(18)	76.46(11)	77.30(15)
O(3)-M(1)-O(1)	91.09(14)	89.78(15)	90.21(11)	90.37(13)
O(3)-M(1)-O(2)	101.01(15)	102.4(2)	102.32(14)	102.06(19)
O(3)-M(1)-N(3)	153.94(15)	151.4(2)	150.30(14)	151.15(19)
O(3)-M(1)-N(4)	88.35(15)	85.2(2)	84.54(14)	85.0(2)
O(4)-M(1)-O(1)	89.92(14)	89.7(2)	89.96(14)	89.76(18)
O(4)-M(1)-O(2)	93.73(15)	90.91(19)	92.40(12)	91.91(15)
O(4)-M(1)-O(3)	106.06(16)	108.2(3)	107.65(15)	107.5(2)
O(4)-M(1)-N(3)	97.05(14)	97.7(2)	99.06(15)	98.58(18)
O(4)-M(1)-N(4)	164.40(14)	163.57(15)	165.20(10)	165.15(14)
N(3)-M(1)-N(4)	70.36(13)	71.8(2)	71.42(14)	71.4(2)

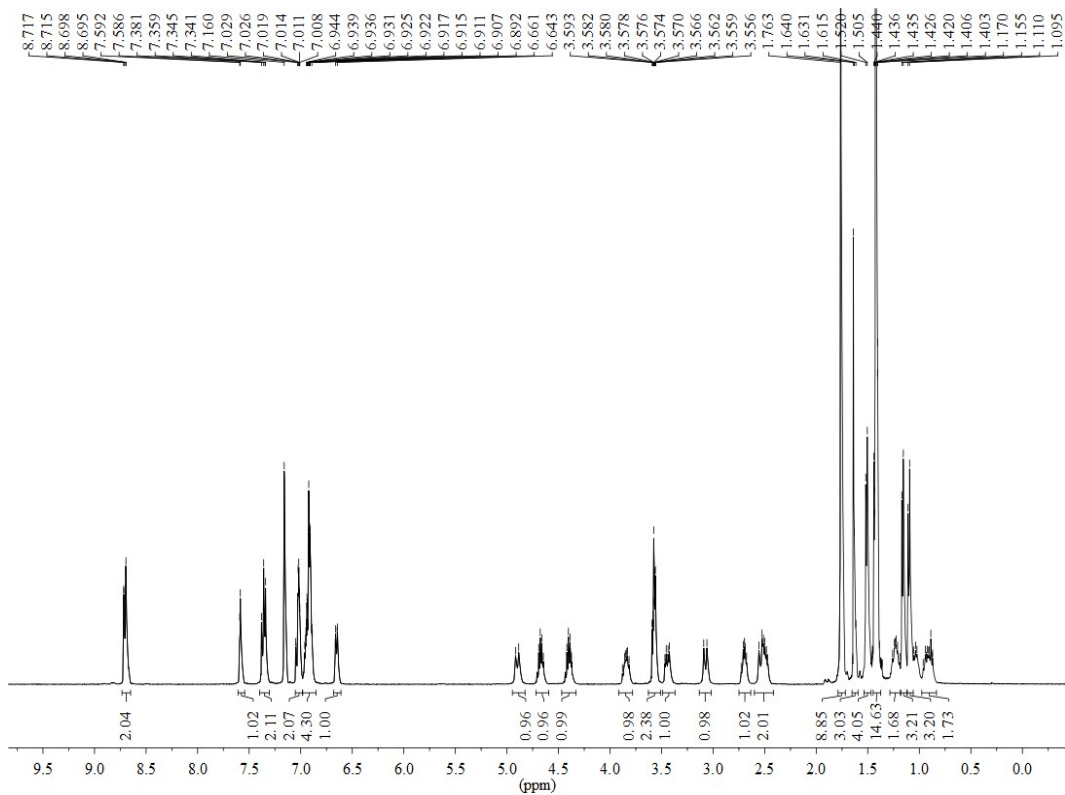


Fig. S1. ^1H NMR spectrum of complex **1** in C_6D_6 at 298 K.

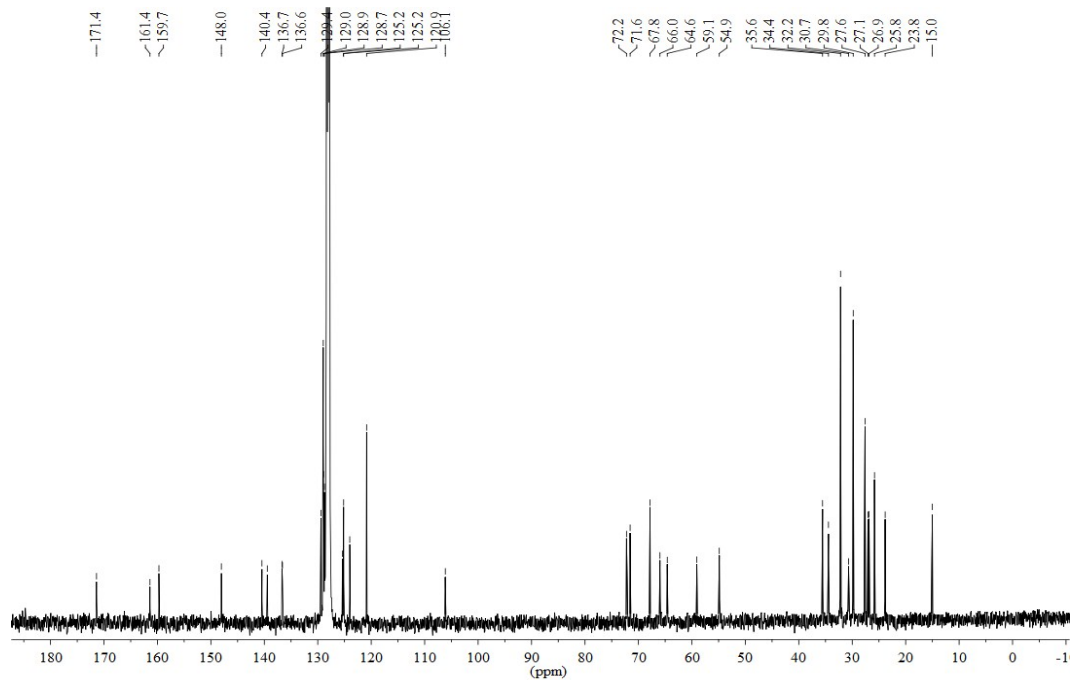


Fig. S2. ^{13}C NMR spectrum of complex **1** in C_6D_6 at 298 K.

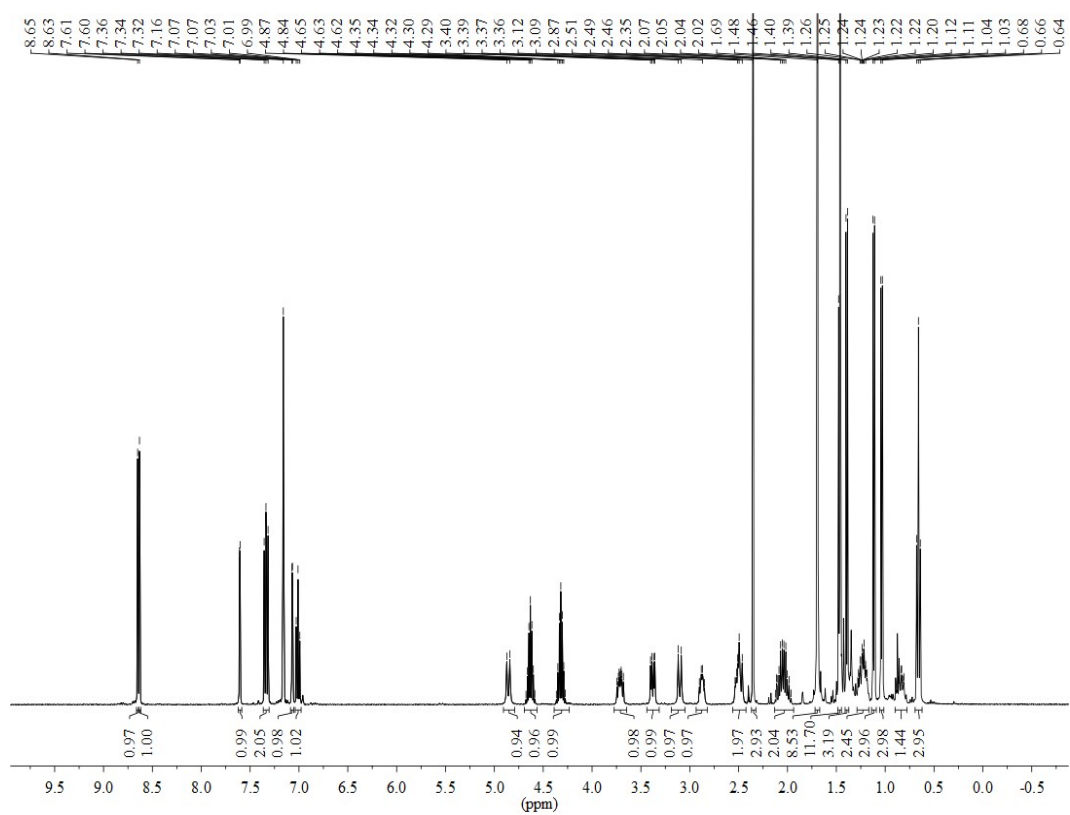


Fig. S3. ^1H NMR spectrum of complex **2** in C_6D_6 at 298 K.

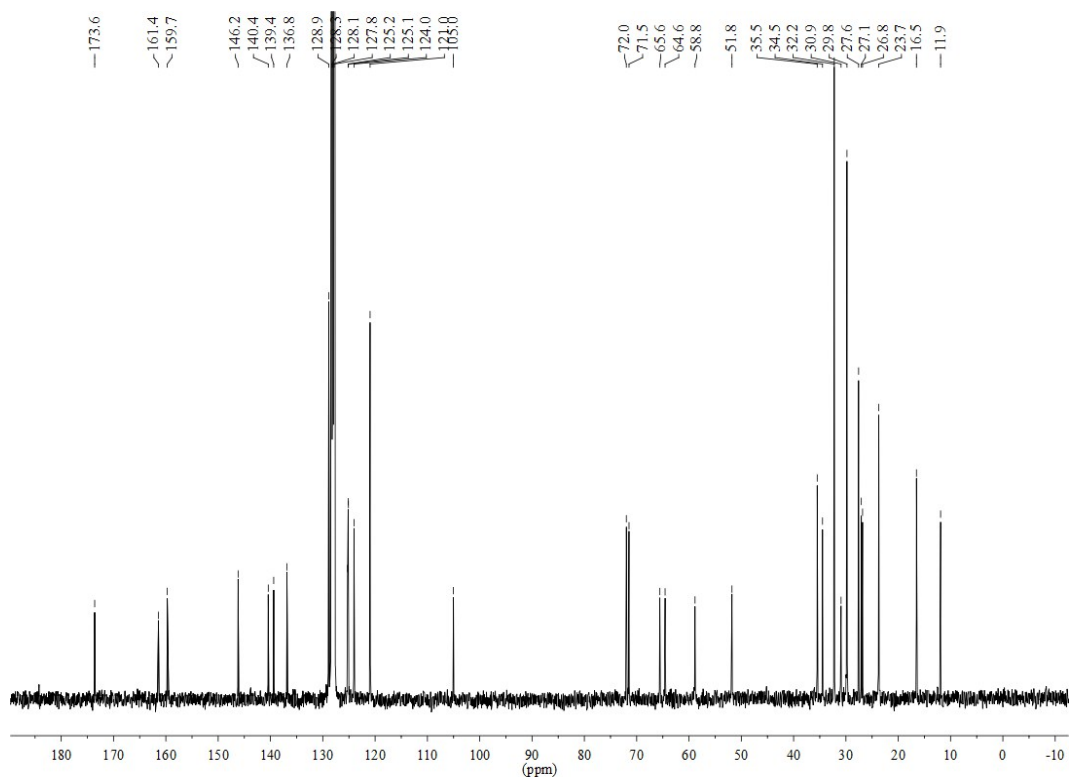


Fig. S4. ^{13}C NMR spectrum of complex **2** in C_6D_6 at 298 K.

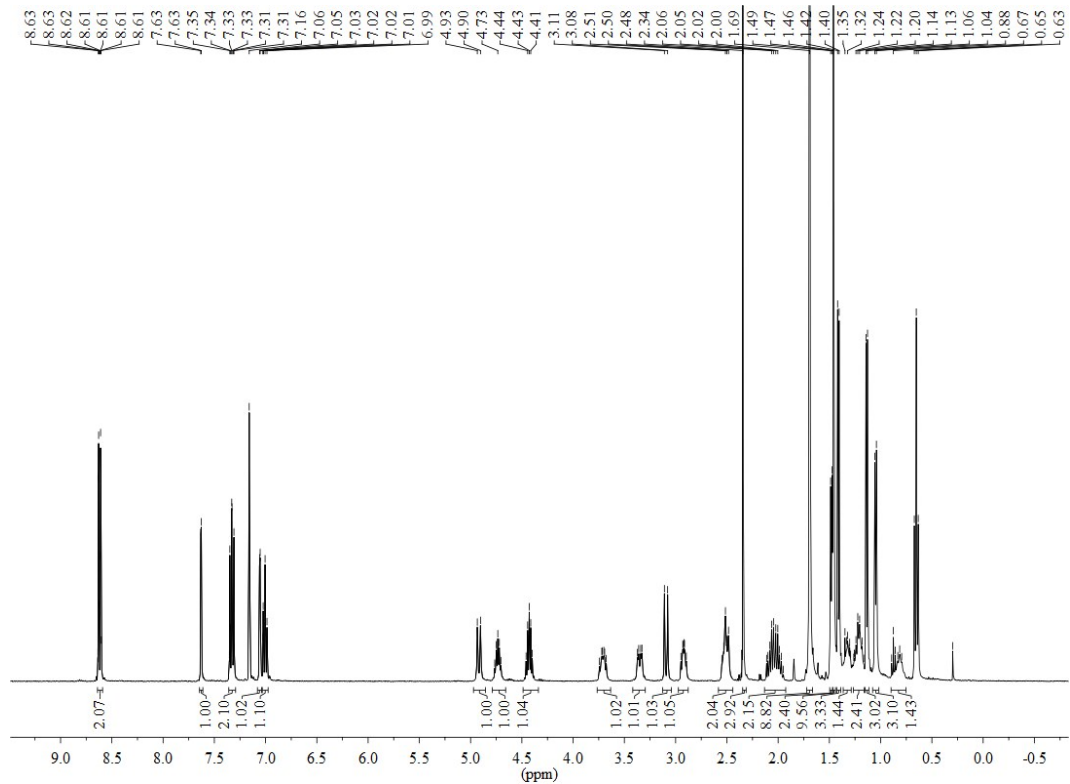


Fig. S5. ^1H NMR spectrum of complex **3** in C_6D_6 at 298 K.

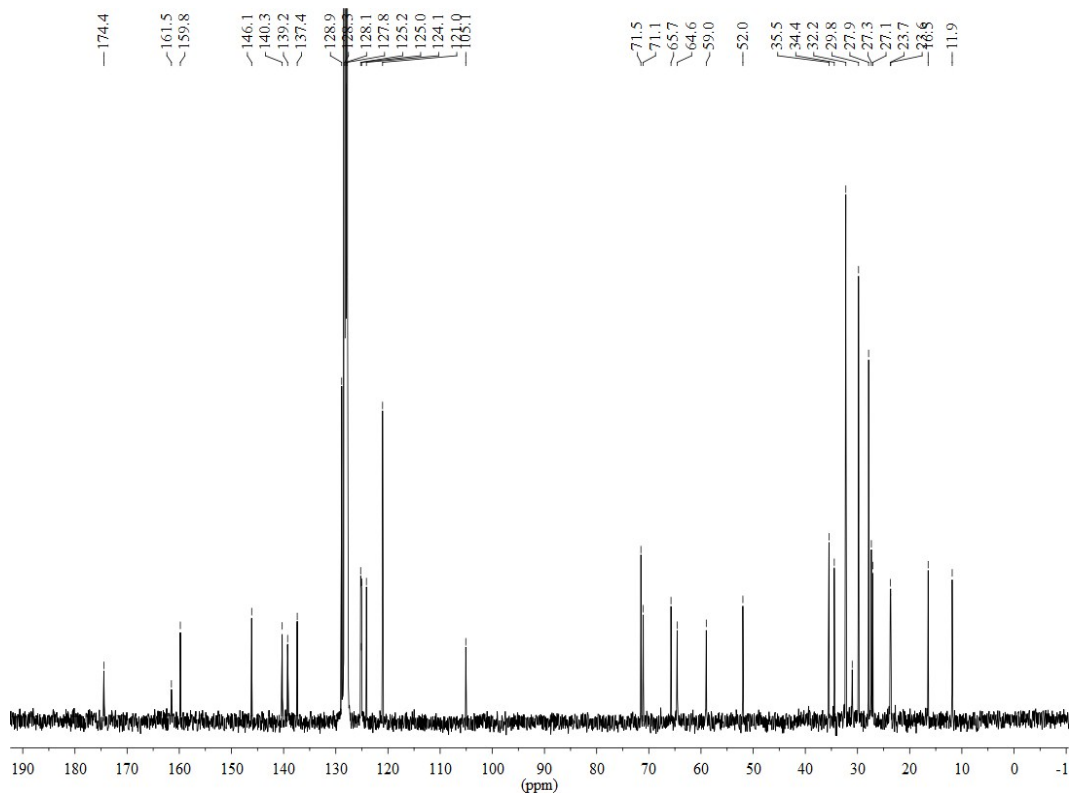


Fig. S6. ^{13}C NMR spectrum of complex **3** in C_6D_6 at 298 K.

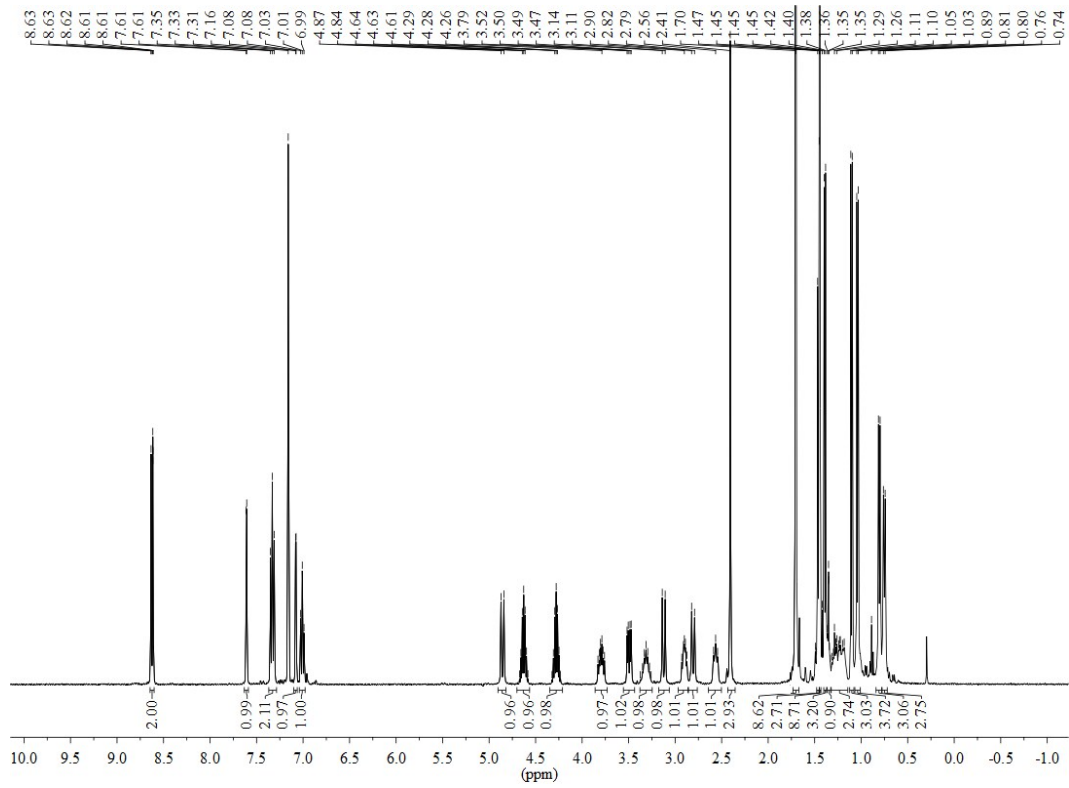


Fig. S7. ^1H NMR spectrum of complex 4 in C_6D_6 at 298 K.

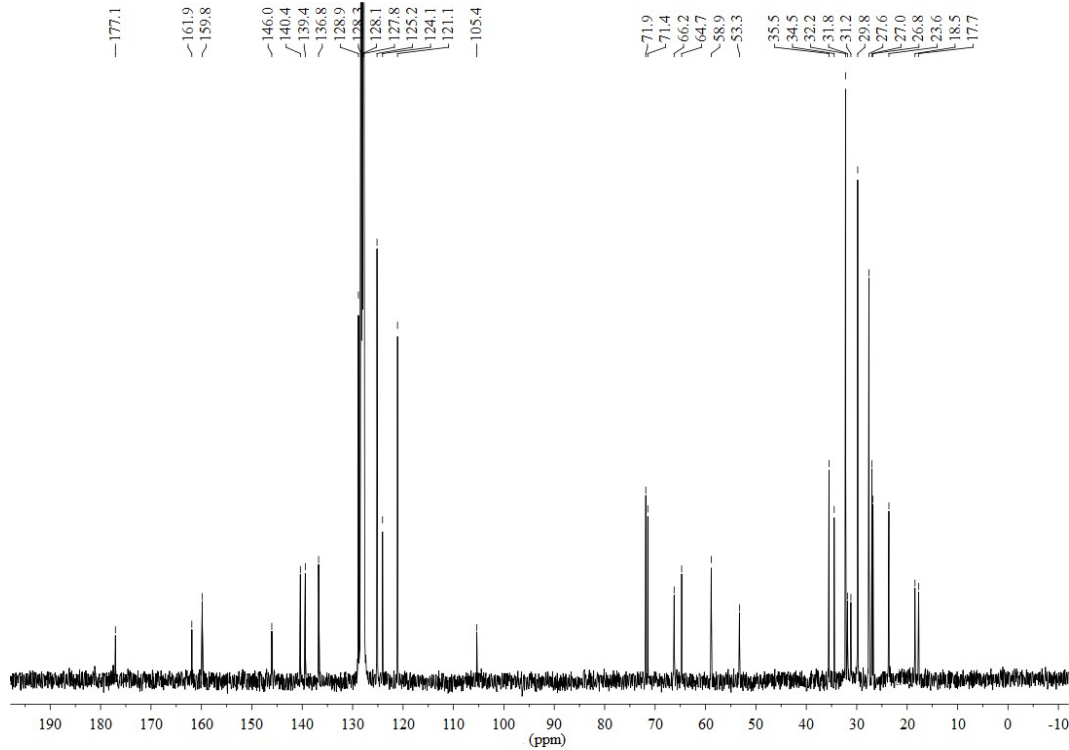


Fig. S8. ^{13}C NMR spectrum of complex 4 in C_6D_6 at 298 K.

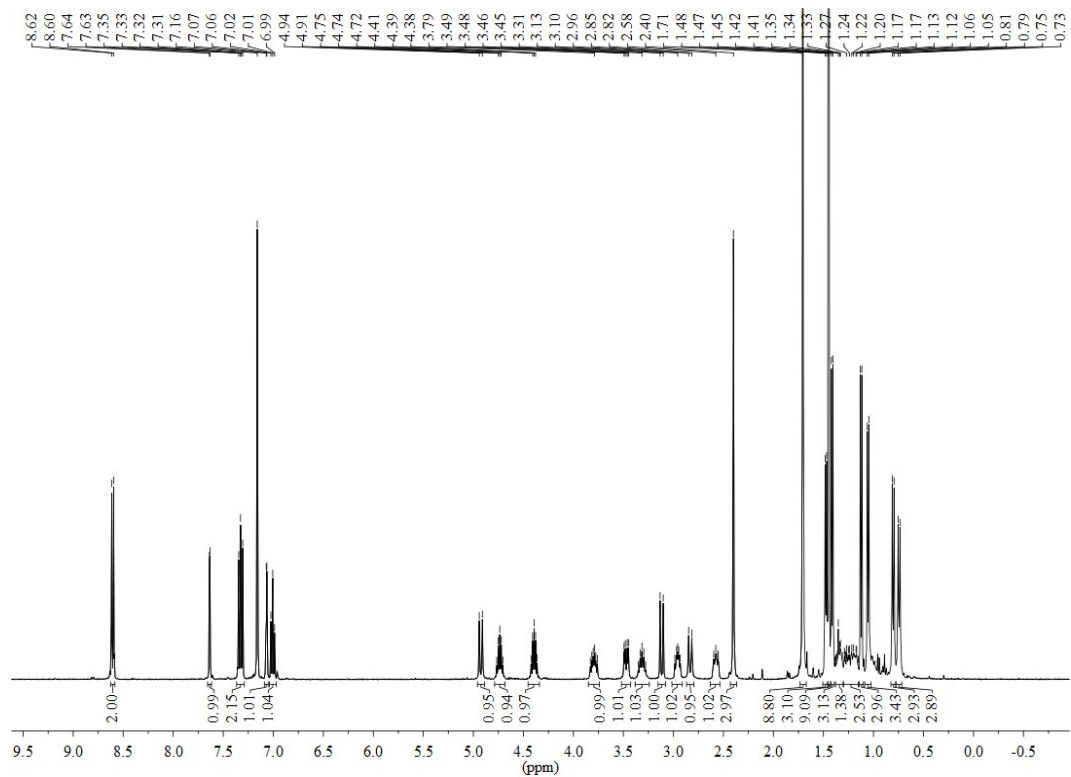


Fig. S9. ^1H NMR spectrum of complex **5** in C_6D_6 at 298 K.

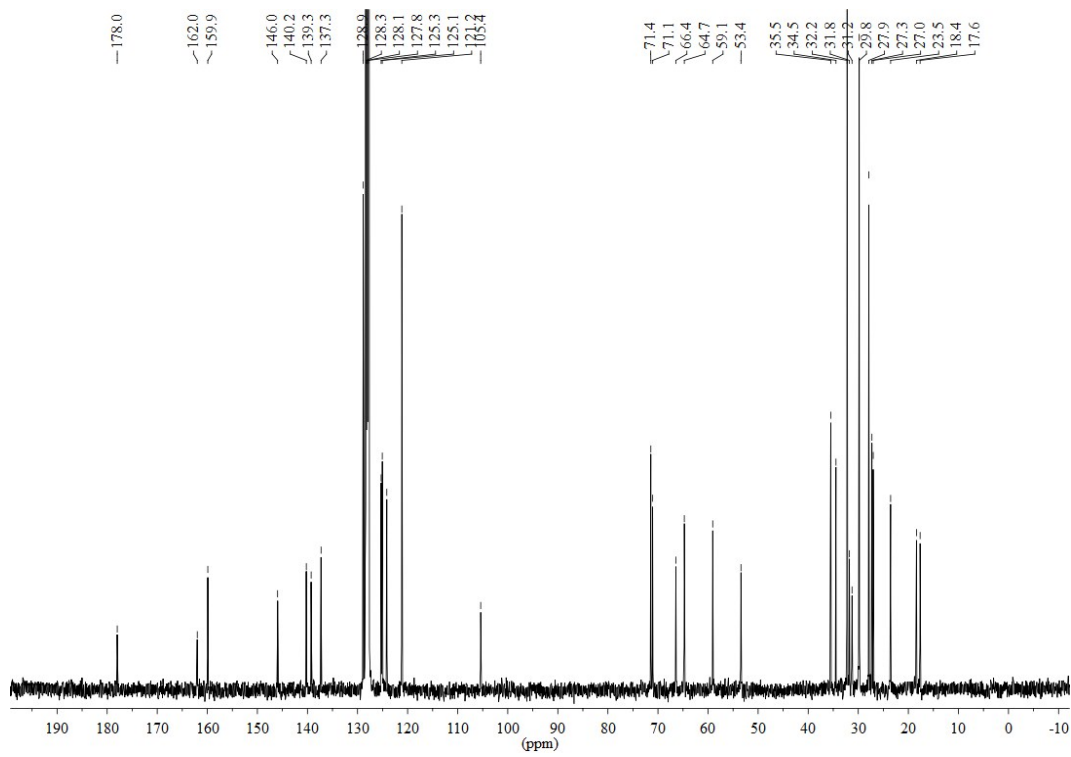


Fig. S10. ^{13}C NMR spectrum of complex **5** in C_6D_6 at 298 K.

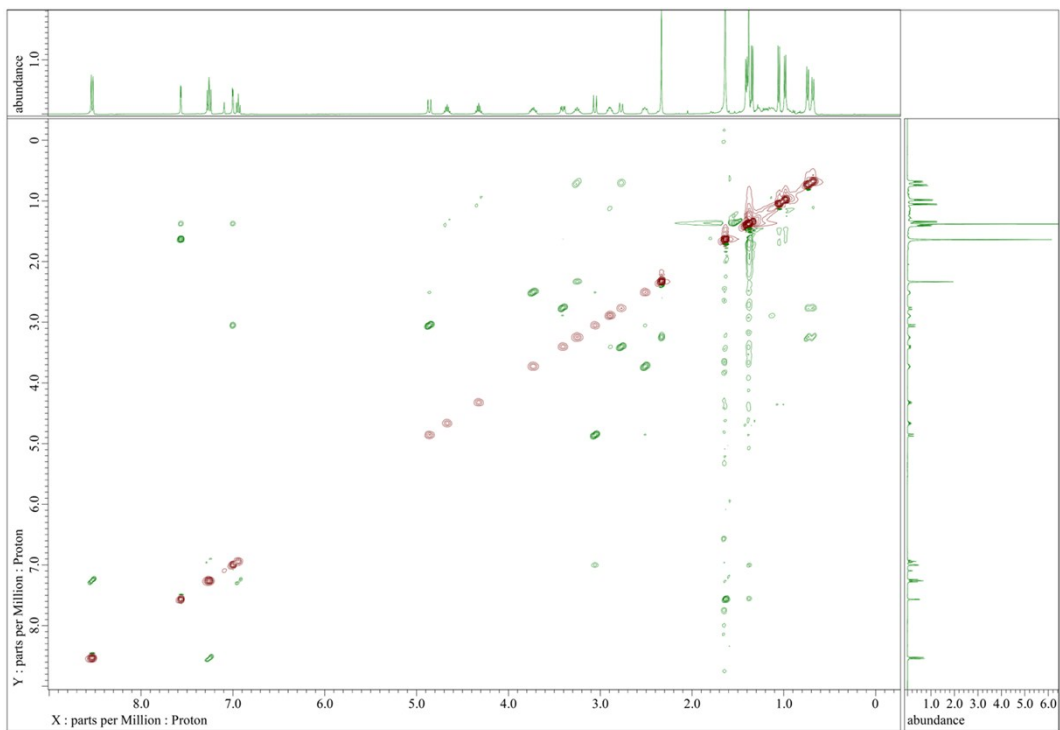


Fig. S11. NOESY spectrum of complex **5** [$\text{L}^3\text{Hf(O}^{\text{i}}\text{Pr)}_2$] in C_6D_6 at 298 K.

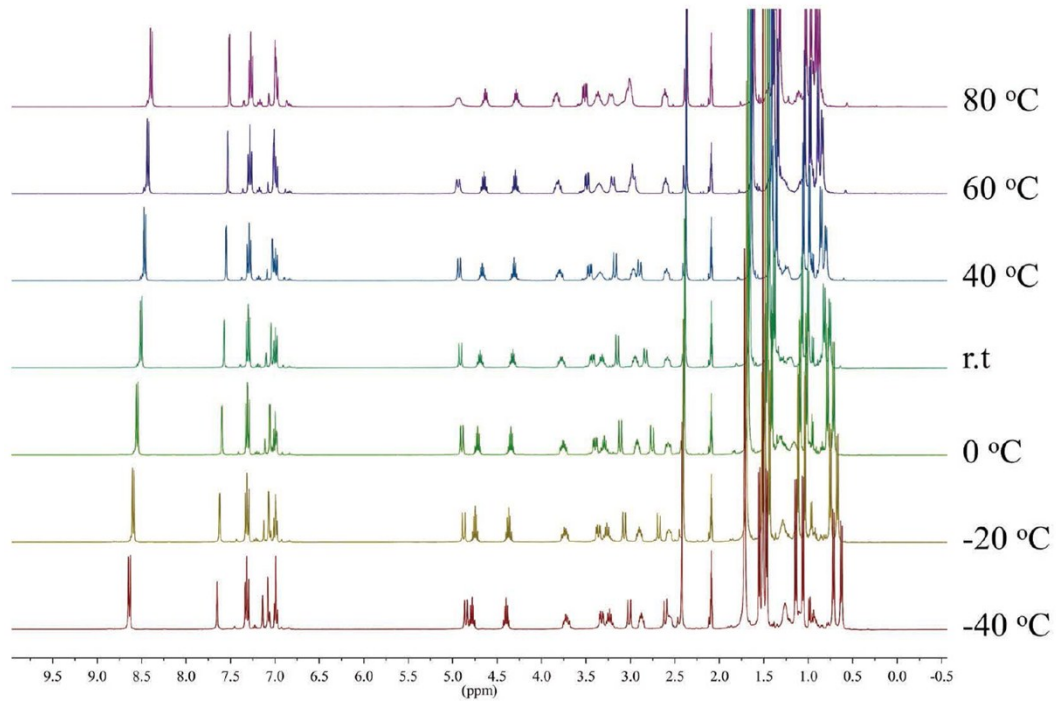


Fig. S12. Variable temperature ^1H NMR spectra for complex **5** in C_7D_8 .

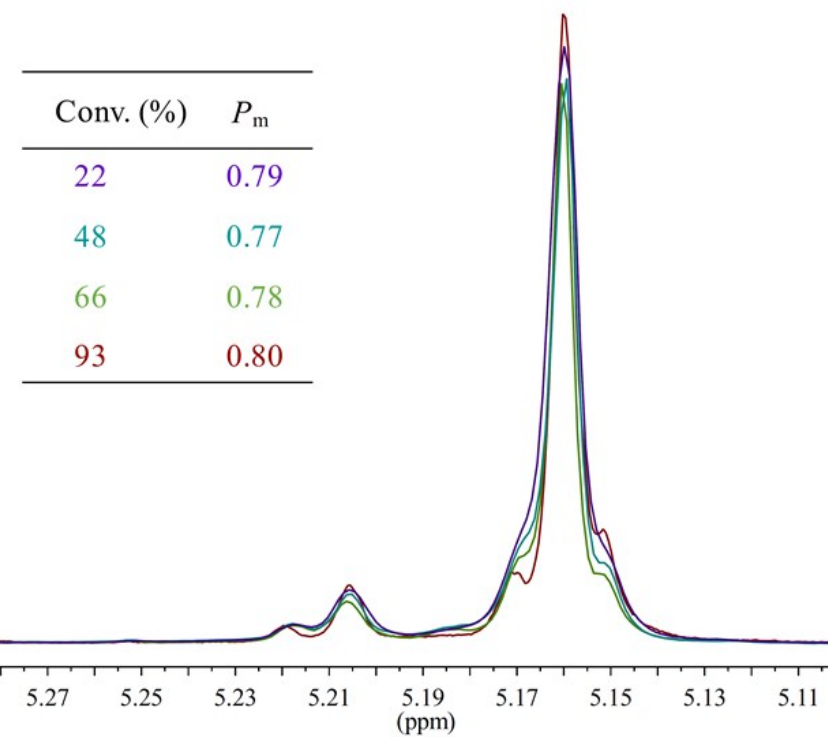


Fig. S13. Methine region of the homonuclear-decoupled ^1H NMR spectra of isotactic PLAs at different conversions produced using initiator **5**.

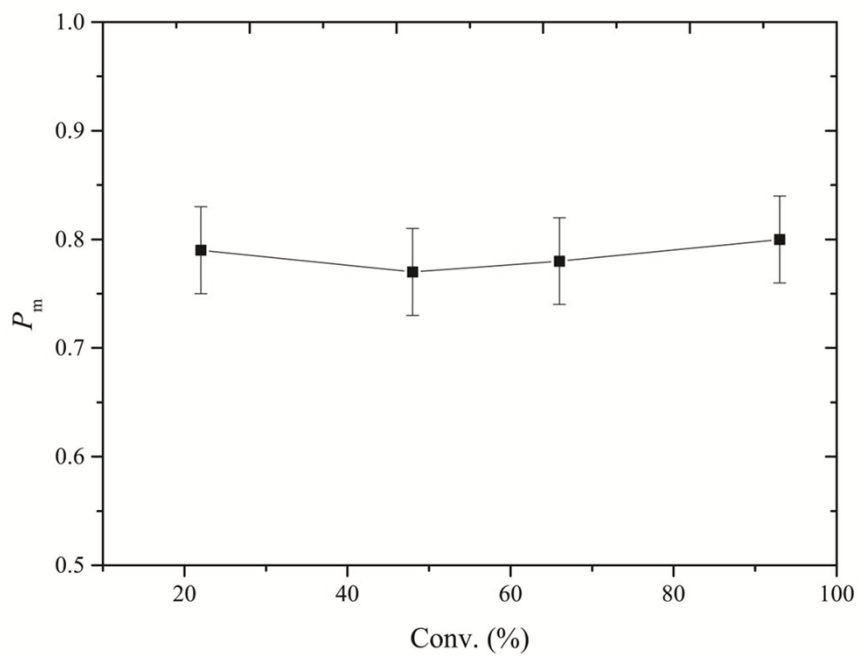


Fig. S14. Plot of P_m vs. conversion for polymerization of *rac*-LA with **5**.

Table S3. Tetrad probabilities based on Bernoullian Statistics (Th) and experimental values (Exp) as obtained by NMR analysis.

Tetrad	Formula	Th	Exp	Th	Exp
		22% conversion		93% conversion	
		$P_m = 0.79$		$P_m = 0.80$	
[mmm]	$P_m^2 + P_r P_m / 2$	0.710	0.710	0.720	0.720
[mmr]	$P_r P_m / 2$	0.083	0.078	0.080	0.076
[rmm]	$P_r P_m / 2$	0.083	0.076	0.080	0.077
[rnr]	$P_r^2 / 2$	0.022	0.021	0.020	0.020
[mrm]	$(P_r^2 + P_r P_m) / 2$	0.105	0.116	0.100	0.111

Table S4. Tetrad probabilities based on Enantiomeric Site Control Statistics (Th) and experimental values (Exp) as obtained by NMR analysis.

Tetrad	Formula	Th	Exp	Th	Exp
		22% conversion		93% conversion	
		$\alpha = 0.87$		$\alpha = 0.87$	
[mmm]	$[\alpha^2 + (1-\alpha)^2 + \alpha^3 + (1-\alpha)^3] / 2$	0.710	0.710	0.710	0.720
[mmr]	$[\alpha^2(1-\alpha) + \alpha(1-\alpha)^2] / 2$	0.057	0.079	0.057	0.076
[rmm]	$[\alpha^2(1-\alpha) + \alpha(1-\alpha)^2] / 2$	0.057	0.078	0.057	0.077
[rnr]	$[\alpha^2(1-\alpha) + \alpha(1-\alpha)^2] / 2$	0.057	0.021	0.057	0.020
[mrm]	$[\alpha(1-\alpha) + \alpha(1-\alpha)] / 2$	0.113	0.116	0.113	0.111

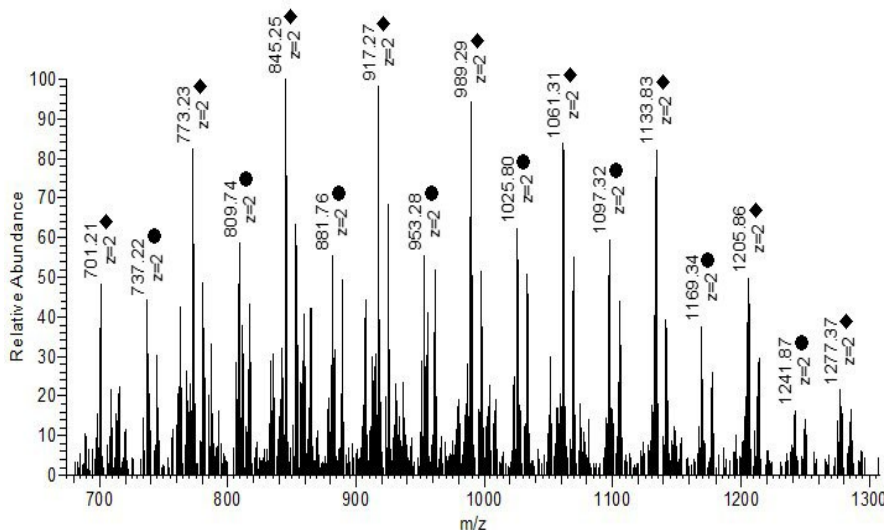


Fig. S15. ESI-MS spectrum of oligomer of *rac*-lactide prepared by complex **5**.